Handling Qualities Analysis of Active Inceptor Force-Feel Characteristics

Carlos A. Malpica
carlos.a.malpica@nasa.gov
NASA Ames Research Center
Moffett Field, CA

Jeff A. Lusardi
jeffery.a.lusardi.civ@mail.mil
US Army Aviation Development Directorate - AFDD
Aviation & Missile Research, Development & Engineering Center
Research, Development and Engineering Command
Moffett Field, CA

Abstract

An analytical model of the coupled pilot/vehicle dynamics, based fundamentally on the classical crossover model of a pilot, was examined extensively for its applicability in studying the effect of inceptor force-feel dynamics. Flight and ground-based simulation tests have been conducted on the AFDD JUH-60A RASCAL and the DLR ACT/FHS EC-135 in-flight simulator helicopters, and the NASA-Ames Vertical Motion Simulator (VMS). Analysis of test data has shown a preference for increased natural frequencies and damping ratios of the simplified second order dynamics of the force-feel system. Correlation of analytical model results with the piloted evaluations from these tests showed that precise handling qualities predictions remain challenging, but that it was possible to qualitatively characterize the relative influence of the force-feel dynamics on the handling qualities as being associated with the neuromuscular coupling of pilot, inceptor and aircraft.

Introduction

Background

The force-feel system characteristics of the cyclic inceptors of most helicopters are function of the characteristics of the components in the mechanical flight control system (mass, springs, friction dampers, etc.). For these helicopters, the force-feel characteristics typically remain constant over the entire flight envelope, with perhaps a trim release for pilots to optionally minimize control forces while maneuvering. With the advent of fly-by-wire control systems and active inceptors in helicopters, the force-feel characteristics are now determined by the closed-loop response of the active inceptor itself as defined by the inertia, force/displacement gradient, damping, breakout force and detent shape configuration parameters in the inceptor control laws. These systems give the flexibility to prescribe different feel characteristics for different control modes or flight conditions, and the ability to provide tactile cueing to the pilot through the actively controlled side-stick or center-stick cyclic inceptor.

For rotorcraft, a few studies have been conducted to assess the effects of cyclic force-feel characteristics on handling qualities in flight. An early study of Ref. 1 provided valuable insight into the static force-deflection characteristics (force gradient) and the number of axes controlled by the side-stick controller for the U.S. Army's Advanced Digital/Optical Control System (ADOCS) demonstrator aircraft. A study on the NASA/Army CH-47B variable-stability helicopter (Ref. 2) provided insight on the significance of cyclic inceptor force-feel dynamic characteristics. This work led to a proposed requirement that set boundaries based on the cyclic natural frequency and inertia, with the stipulation of a lower damping ratio limit of 0.3 (Ref. 3). Another study was conducted by the NRC Institute for Aerospace Research of Canada using their variable-stability Bell 205A helicopter (Ref. 4). This research suggested boundaries for stick dynamics based on natural frequency and damping ratio. While these two flight test studies produced boundaries for acceptable and unacceptable stick dynamics for rotorcraft, they were not able to provide guidance on how variations of the stick dynamics in the acceptable region impact handling qualities.

More recently, a ground based simulation study (Ref. 5) suggested little benefit was to be obtained from variations of the damping ratio for a side-stick controller exhibiting high natural frequencies (greater than 17 rad/s) and damping ratios (greater than 2.0). A flight test campaign was conducted concurrently on the RASCAL JUH-60A in-flight simulator and the ACT/FHS EC-135 in-flight simulator (Ref. 6 and 7). Upon detailed analysis of the pilot evaluations the study identified a clear preference for a high damping ratio and natural frequency of the center stick inceptors. Handling

Presented at the AHS 69th Annual Forum, Phoenix, Arizona, May 21–23, 2013.

qualities for side stick controllers were found to be less dependent on the damping.

These recent studies have compiled a substantial amount of data, in the form of qualitative and quantitative pilot opinion. However, clear design guidance is still found to be lacking. The studies of Ref. 6 and 7 compared the handling qualities with the short-term attitude response specification criteria of ADS-33 (Ref. 8), applied to the force input. Discrepancies with the assigned handling qualities showed that proposed analytical design metrics, or criteria, were not suitable to accurately predict the handling qualities. A preliminary comparison using a model-based pilot analysis technique had also been conducted in Ref. 6, concluding that further analysis to include the effect of motion cueing on the pilot model was required.

Objectives

The overall goal of the present study is to develop a fundamental understanding of the primary underlying mechanisms associated with helicopter inceptor force-feel dynamics that govern the handling qualities through the use of an analytical pilot model.

Approach

For this purpose the analysis of the handling qualities results from flight and ground-based simulation testing by means of the model-based pilot/vehicle methodology of Refs. 9–11 was extended. Particular emphasis was placed on analyzing the effects of motion cueing on the pilot compensation. The expanded analysis included comparison with Mission Task Elements not previously assessed in Ref. 6.

Analytical Model

Structural Pilot Model

The block diagram shown in Figure 1 illustrates the single axis feedback structure proposed by Hess (Ref. 10), and is employed at the core of the analytical model adopted in this study. The model accounts, in a simple form, for the fundamental feedback mechanisms which the human pilot relies on for classical regulatory compensation. The sub-components of the structural pilot model include the neuromuscular dynamics (Y_{NM}), the proprioceptive and vestibular feedback (Y_{PF} and $sK_{\dot{m}}$ respectively), and the visual error compensation (Y_e). Hess argues that the primary ability of the human pilot to effect compensation over the aircraft is through the proprioceptive sensing of the controller displacement input. The proprioceptive feedback element in Figure 1 is therefore central to the philosophy of the structural model, and represents, in essence, a pilot's "internal model" of the aircraft dynamics such that the fundamental principles of the classical crossover frequency model of a human pilot

$$\frac{M}{E} = Y_P Y_C \approx \frac{\omega_c}{s} e^{-\tau_e s}$$

are observed. Another key feature in the structural pilot model is the inclusion of the inceptor dynamic response to pilot force inputs (Y_{FS}) inside of the proprioceptive feedback loop. This allows, as exemplified in Reference 8, for this modeling approach to be of use in the analysis of the handling qualities impact of the inceptor dynamics.

In terms of Figure 1, the vehicle output M generally represents any vehicle degree of freedom. Command input C represents the input or desired value of M. The error E corresponds to the visually sensed difference between the two quantities. Output of the neuromuscular representation is a force input δ_F which drives inceptor displacement output δ. Finally, U_M is the proprioceptive feedback signal, which, as will be discussed shortly is critical to the handling qualities prediction method.

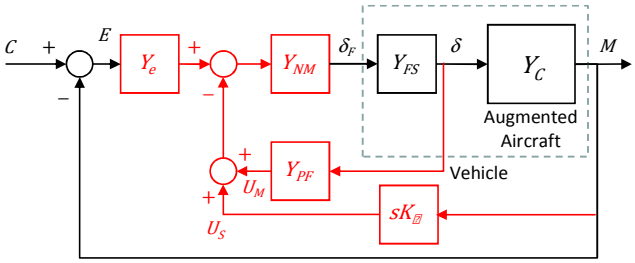

Figure 1: Structural Pilot/Vehicle Model

Handling Qualities Analysis

The structural model was demonstrated in Reference 11 to be ideally suited to the analysis of task requirements in terms of aggressiveness, performance and predicted handling qualities. The theory behind the structural model of Figure 1 suggests the pilot's perception of the handling qualities is dependent on the 'power' in the proprioceptive feedback signal $u_M(t)$. It was therefore proposed that handling qualities are reflected by the magnitude of a Handling Qualities Sensitivity Function (HQSF), defined as

$$HQSF = \left| \frac{U_M}{C}(j\omega) \cdot \frac{1}{K_e} \right|. \qquad (1)$$

Here K_e is the proportional component of the visual compensation strategy, and the HQSF is defined by the transfer function between the proprioceptive feedback signal U_M and the commanded input C. If the model is applied to attitude regulation, e.g., then the HQSF is in essence an indication of the power in the proprioceptive compensation that may be elicited of the pilot model in response to the attitude changes demanded by a given maneuver.

The prediction of handling qualities is predicated on the HQSF from Eq. (1) being bounded from above by a prescribed set of boundaries shown in Figure 2, over the typical frequency range of pilot control, i.e., 1–10 rad/s. The handling qualities predictions from this model approach can be tailored to different task aggressiveness required. This is achieved by selecting an appropriate

pilot crossover frequency. The use of the HQSF in the context of task analysis has been well illustrated in Ref. 11. The reader is referred to that work for a detailed explanation.

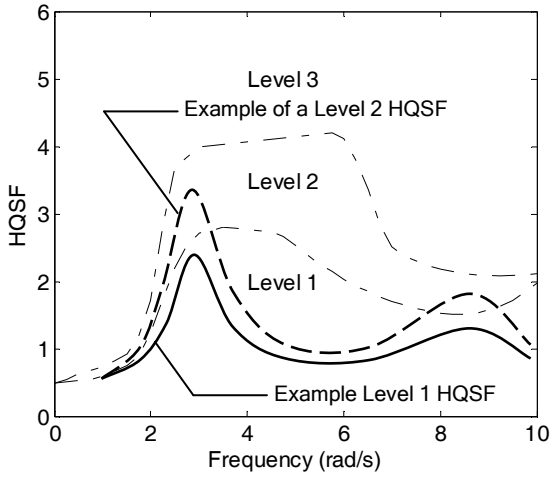

Figure 2: HQSF level boundaries

One of the difficulties in using model-based measures such as the HQSF for handling qualities prediction is that the validity of boundaries proposed in the literature is usually subject to a specific set of assumptions or conditions, such as the value of crossover frequency or a specific set of configuration parameters. While the work of Ref. 11 accommodated variable crossover frequencies, results were predicated on a unique set of configuration parameter values, in particular the omission of vestibular feedback. This is because, according to Hess, the structural model was set up for HQ predictions under some fairly rigorous (and somewhat simplified) ground rules: (a) particular model feedback structure, (b) no variations in neuromuscular model and pilot time delays, and (c) no vestibular feedback. These ground-rules and pilot model limitations allowed a fairly simple metric, i.e., the HQSF to reflect handling qualities levels. In this paper the handling qualities will be compared to the specified boundaries only when conditions (a)–(c) apply.

Model Configuration

Figure 3 illustrates the pilot/vehicle model structure for lateral and longitudinal position control tasks that was employed herein. The fundamental structure relies on the structural pilot model for the inner-loop control of vehicle attitudes, in both pitch and roll. The outer feedbacks close the loop on the lateral and longitudinal vehicle positions. The omission of yaw and heave control axes is, of course, a simplification, but this can be justified by the use of Heading Hold and Altitude Hold in hover and Velocity Hold at high speed that were employed in flight and simulation.

Given the vehicle dynamics and an estimate of the crossover frequencies for each axis, the remaining step is to configure the values of the different elements of the pilot model, i.e., Y_{P_x}, Y_{P_y}, Y_{P_ϕ} and Y_{P_θ}.

The selection of parameter values and configuration procedures followed in this paper for the baseline pilot/vehicle model have been documented in exhaustive detail by Hess et al. in Reference 11. This choice provided a documented basis for validation of the model and represent, overall, "good practice" values that are supported by a significant body of research. These are summarized briefly in the following sections.

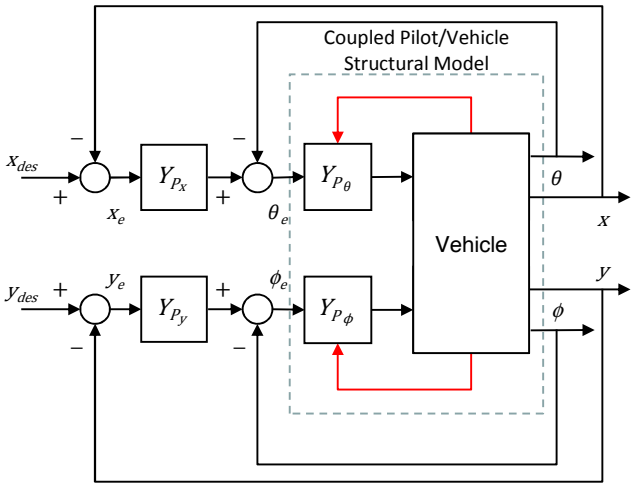

Figure 3: MIMO pilot/vehicle system for position control tasks

Baseline model parameters

Neuromuscular dynamics: Nominal pilot neuromuscular system dynamics were chosen from Ref. 11 for both control axes. These are represented by the normalized second order transfer function

$$Y_{NM} = \frac{10^2}{s^2 + 2(0.707)10s + 10^2}.$$

Vestibular feedback: Vestibular feedback is not included in the baseline configuration since the work available in the literature upon which the handling qualities prediction method is built has been entirely based on fixed-base simulation activities. Consequently the pilot's gains on motion cueing are both set to zero.

$$K_{\dot{\phi}} = K_{\dot{\theta}} = 0$$

Proprioceptive feedback: Selection of the proprioceptive feedback is stated in Ref. 11 to be a critical choice and follows one of the following three forms

$$Y_{PF} = \begin{cases} \dfrac{K}{s+a} \\ K \\ K(s+a) \end{cases}$$

Reference 11 also dictates that K be chosen such that the minimum damping ratio of any oscillatory closed-loop proprioceptive system poles be 0.15. The value of a is then chosen generally such that $Y_{PF} \propto sY_C$ in the vicinity of the crossover frequency in each axis.

Inner-loop attitude compensation: Visual attitude error compensation, in both axes, was defined to be of the general form

$$Y_e = K_e\left(1+\frac{\varepsilon}{s}\right)e^{-\tau_0 s}$$

with τ_0=0.2 s defining the nominal configuration. The value of the integral gain ε is selected to ensure the proper magnitude and phase of the open-loop transfer function in the low frequency range. The coefficients K_{ϕ_e} and K_{θ_e} defining the visual compensation gains on perceived roll and pitch attitude error are configured to ensure ω_{c_ϕ} and ω_{c_θ} crossover frequencies.

Outer-loop position compensation: The pilot longitudinal and lateral outer-loop compensation elements were selected as the lead compensators

$$Y_{P_x} = K_{P_x}\frac{s-z}{s-p} \quad \text{and} \quad Y_{P_y} = K_{P_y}\frac{s-z}{s-p} \qquad (2)$$

with $z = -0.1$ and $p = -5.0$. The outer-loop gains are selected to ensure crossover frequency separation, that is, $\omega_{c_y} = \omega_{c_\phi}/3$ and $\omega_{c_x} = \omega_{c_\theta}/3$.

Crossover frequency selection

The pilot crossover frequency effectively serves as the one independent tuning parameter to the model. A crossover frequency of 2 rad/s can generally be specified as a nominal representation of the pilot operating frequencies. Alternatively, crossover frequencies can be estimated from either an inverse dynamic analysis or from experimentally derived measurements of pilot control inputs. The advantage of the inverse dynamic analysis procedure is that it allows for the estimation of pilot crossover frequencies without a priori information, other than a description of the maneuver to be executed.

For this paper, the crossover frequencies were estimated from inner-loop attitude command response time histories obtained from the inverse dynamic analysis procedure described in Ref. 11, as follows

$$\omega_{c_\phi} \approx 2.4\frac{\Delta\dot{\phi}_{max}}{\Delta\phi_{max}} \quad \text{and} \quad \omega_{c_\theta} \approx 2.4\frac{\Delta\dot{\theta}_{max}}{\Delta\theta_{max}}$$

This relationship was suggested in Ref. 12 for use in the analysis of helicopter pilot performance for individual short-term discrete maneuvers.

Experimental Data

Correlation of the analysis technique was achieved through comparison with results from flight and simulation tests. Testing conducted on the RASCAL JUH-60A and ACT/FHS EC-135 in-flight simulators was described in detail in Ref. 6. A follow-on pilot-in-the-loop test was conducted in the NASA Ames Vertical Motion Simulator (VMS) (Ref. 13) as an extension of the flight test study of Ref. 6. Experimental test pilot handling qualities ratings and quantitative performance and aircraft state data are available from this set of flight and simulation tests. The simulation experiment provided an opportunity to evaluate the effect of motion cues on the handling qualities predictive criteria and piloted control for the particular set of inceptor force-feel characteristics. Additionally, the trials evaluated an expanded matrix of inceptor damping ratios and natural frequencies, with both a center-stick and side-arm cyclic controllers.

Test Overview

Flight testing conducted on the RASCAL JUH-60A and the ACT/FHS EC-135 in-flight simulators was described in detail in Refs. 6 and 7. For the VMS study, the RASCAL control laws and safety monitors of the flight tests were implemented with the GenHel UH-60A math model for the aircraft. A light level of turbulence was simulated using a CETI model (Ref. 14) to replicate flight test conditions. The cockpit was configured to match the UH-60 cockpit as necessary to provide the required visual cueing needed to perform evaluations and collect handling qualities ratings (HQRs). The McFadden force loader controls in the VMS were set to replicate the active center-stick cyclic currently installed in the RASCAL, and also utilized an active side-arm controller to allow for comparative evaluations of these two different inceptors.

Experimental Force-Feel Configurations

The cyclic inceptor dynamics of Ref. 6 maintained the same force displacement gradient of 0.75 lb/in for all configurations. In addition, the breakout force was set at 1 lb, and a small detent was added for testing with Attitude Command. The experiment tested the various force-feel configurations listed in Table 1 for both Attitude and Rate Command response types. Force-feel configurations A, D and F were also tested in the VMS trials, in addition to a high damping configuration F_H defined by a nominal 8 rad/s natural frequency and damping ratio of 2.0.

Table 1: Nominal Force-Feel Configurations of Ref. 6

Configuration	Bandwidth (rad/s)	Damping Ratio
A	7	1.5
B	23	1.5
C	23	0.7
D	7	0.7
F	9	0.9

Aircraft Model

Low order transfer function approximations of the aircraft pitch and roll rate dynamics were used in the structural pilot/vehicle model. These were synthesized to match measured frequency responses obtained from piloted sweeps using frequency-domain identification techniques (Figures 5-8(a)). Models were matched to a reasonable accuracy in the range 0.2–10 rad/s, which is sufficient for handling qualities analysis.

Transfer functions modeling the two horizontal inertial velocity responses to pilot input were constructed from the attitude responses, as follows

$$\frac{V_x}{\delta_{lon}(s)} = -\frac{g}{s - X_u} \cdot \frac{\theta}{\delta_{lon}(s)} \cdot H_\theta(s)$$

and

$$\frac{V_y}{\delta_{lat}}(s) = \frac{g}{s - Y_v} \cdot \frac{\phi}{\delta_{lat}}(s) \cdot H_\phi(s)$$

Here $H_\theta(s)$ and $H_\phi(s)$ are introduced to account for any higher order modes in the response. Values for the stability derivatives X_u and Y_v, and transfer functions $H_\theta(s)$ and $H_\phi(s)$ were then identified to match the measured frequency responses in the aforementioned frequency range (Figures 5-8(b)). Transfer functions describing the helicopter attitude and translational response dynamics are listed in Table 2, below.

Table 2: Low Order Equivalent System (LOES) transfer function approximations of aircraft dynamics

Rate Command
$\frac{\phi}{\delta_{lat}} = \frac{716.6946}{s(s^2 + 11.02s + 80.52)} e^{-0.047s}$
$\frac{V_y}{\delta_{lat}} = \frac{3.2681(s+6)(s^2 - 3.14s + 246.5)e^{-0.047s}}{s(s+0.164)(s+12)(s^2 + 11.02s + 80.52)}$
$\frac{\theta}{\delta_{lon}} = \frac{536.5482}{s(s^2 + 9.147s + 55.67)} e^{-0.11s}$
$\frac{V_x}{\delta_{lon}} = \frac{-50.4477\ (s^2 + 0.4622s + 6.612)}{s(s+0.048)(s^2 + 9.147s + 55.67)} e^{-0.11s}$
Attitude Command
$\frac{\phi}{\delta_{lat}} = \frac{550.0807}{(s+1.622)(s+31.83)} e^{-0.19s}$
$\frac{V_y}{\delta_{lat}} = \frac{6.923(s+2.868)(s^2 - 2.581s + 76.57)e^{-0.19s}}{(s+0.094)(s+1.622)(s+5.659)(s+31.83)}$
$\frac{\theta}{\delta_{lat}} = \frac{25.2989}{(s+1.355)(s+3.766)} e^{-0.14s}$
$\frac{V_x}{\delta_{lon}} = \frac{-2.3242(s^2 + 0.1086s + 6.998)}{(s+0.064)(s+1.355)(s+3.766)} e^{-0.14s}$

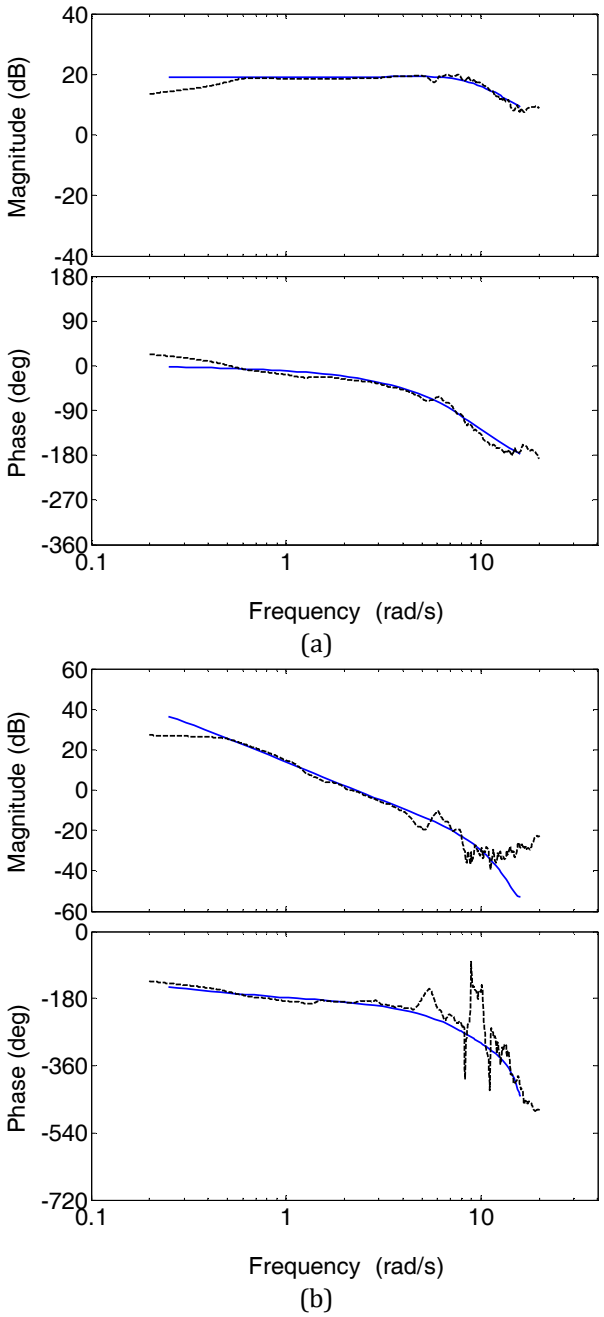

Figure 4: Low order equivalent approximations of frequency response to pilot displacement input, lateral axis, RC: (a) roll rate, (b) velocity

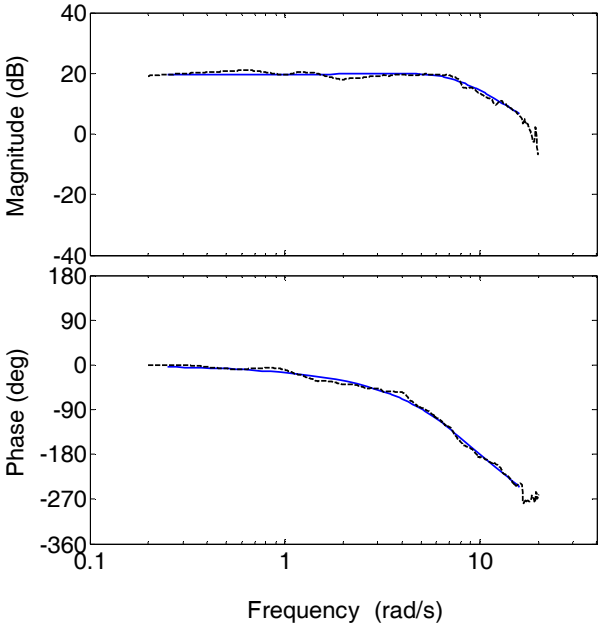

(a)

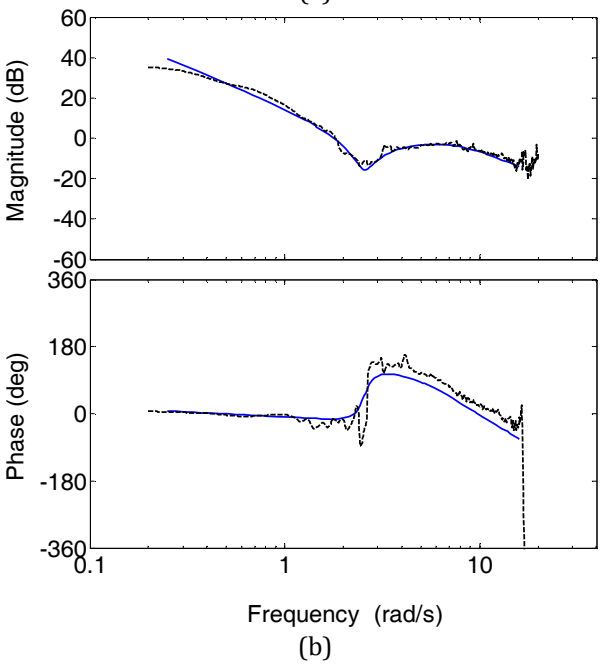

(b)

Figure 5: Low order equivalent approximations of frequency response to pilot displacement input, longitudinal axis, RC: (a) pitch rate, (b) velocity

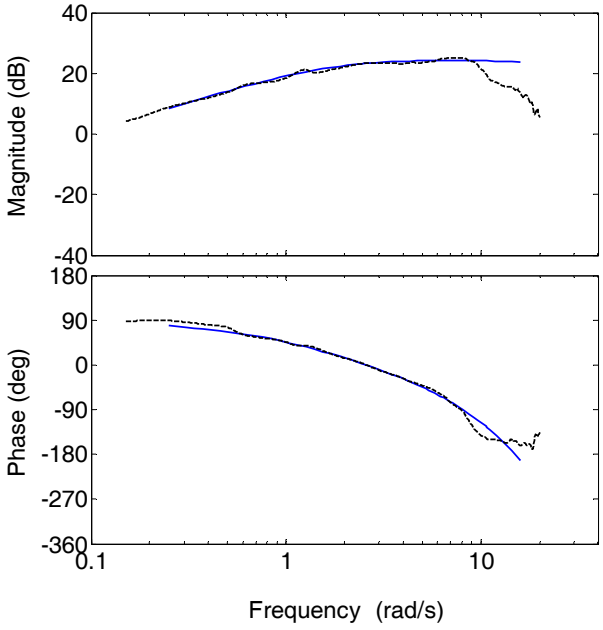

(a)

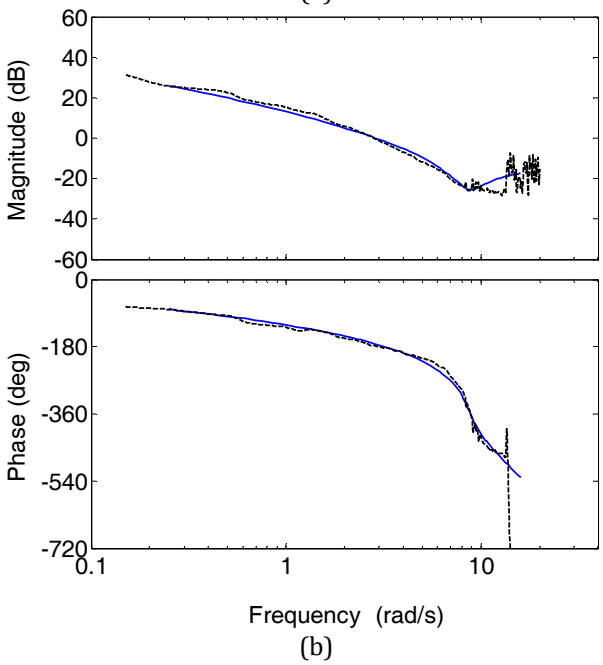

(b)

Figure 6: Low order equivalent approximations of frequency response to pilot displacement input, lateral axis, AC: (a) roll rate, (b) velocity

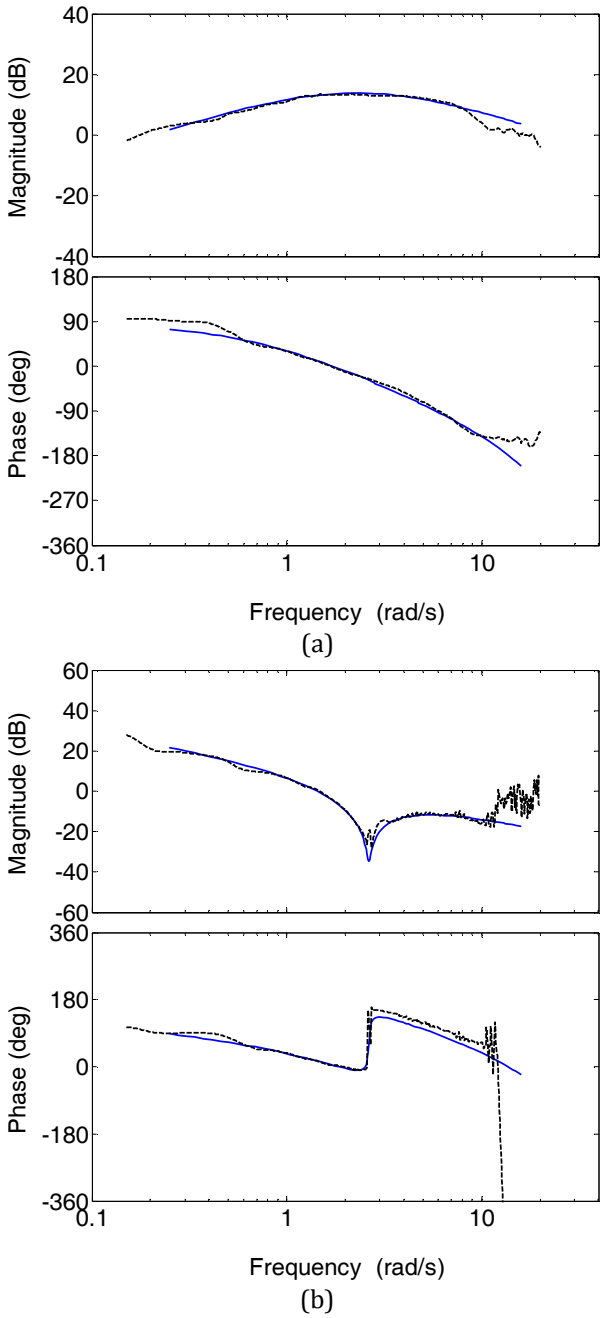

Figure 7: Low order equivalent approximations of frequency response to pilot displacement input, longitudinal axis, AC: (a) pitch rate, (b) velocity

Evaluation Tasks

Two mission task elements (MTEs) from ADS-33E were used for evaluation of the effects of cyclic force feel characteristics on handling qualities, the Hover MTE, and the Slalom MTE. The Hover MTE is a low speed maneuver (6-10 kt) that requires the pilot to make small inputs around trim. The Slalom MTE is a high speed maneuver (60 kt) that requires the pilot to make low frequency, large amplitude inputs. Together, the tasks are ideally suited to evaluate cyclic force feel characteristics for inputs that are broadly representative of control strategies utilized by helicopter pilots.

Piloted Evaluations

Handling Qualities Ratings

Pilot Handling Qualities Ratings from the ground-based VMS experiment and flight testing on the JUH-60A RASCAL were found to compare rather favorably. For the Slalom MTE, ratings for the three force-feel configurations and the Rate Command response type, shown in Figure 8, indicated borderline Level 1/2 handling qualities. For the same force feel configurations in Attitude Command, Level 1 handling qualities were attained. The Handling Qualities Ratings from the Hover MTE evaluations are shown in Figure 9. With the exception of Rate Command case F, all force-feel cases were evaluated, on average, within a difference of 1 HQR.

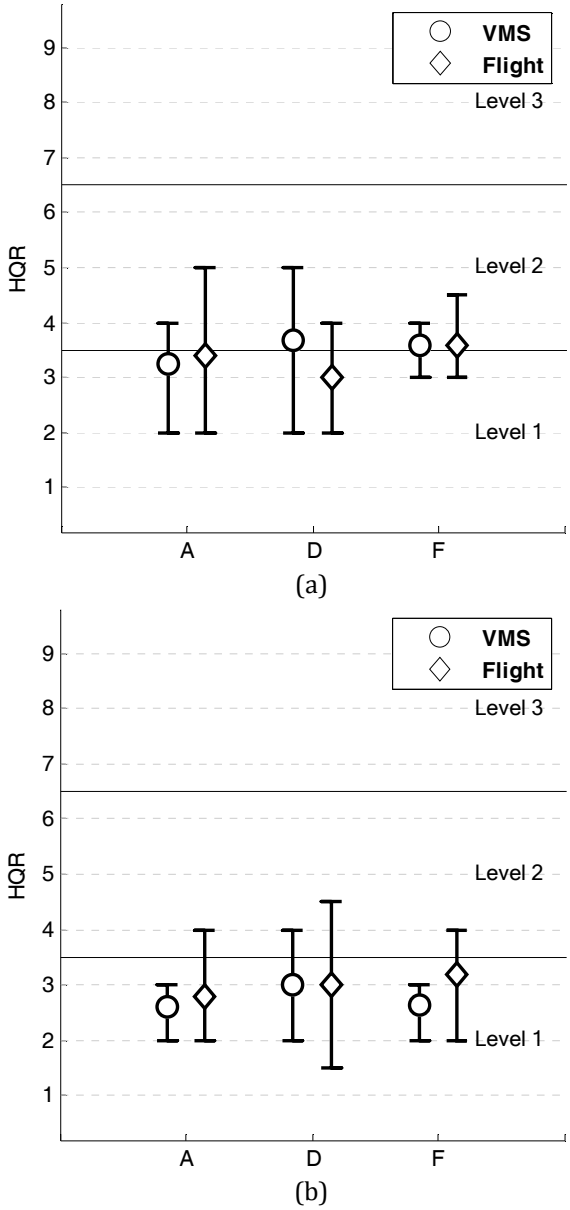

Figure 8: Comparison of Handling Qualities Ratings from VMS and flight testing (Slalom MTE, Center Stick): (a) Rate Command, and (b) Attitude Command

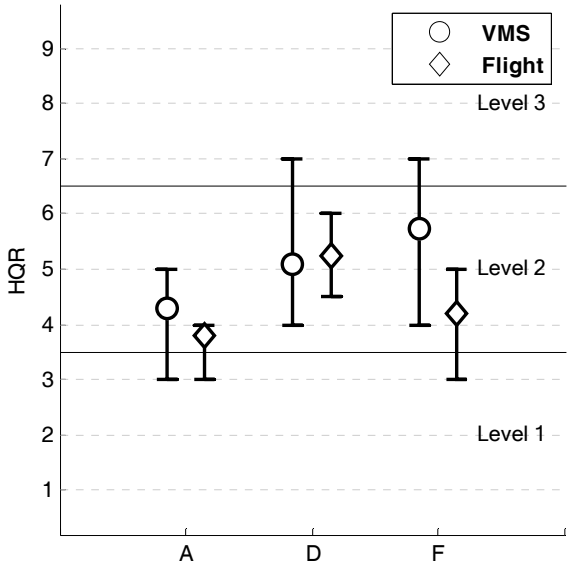

(a)

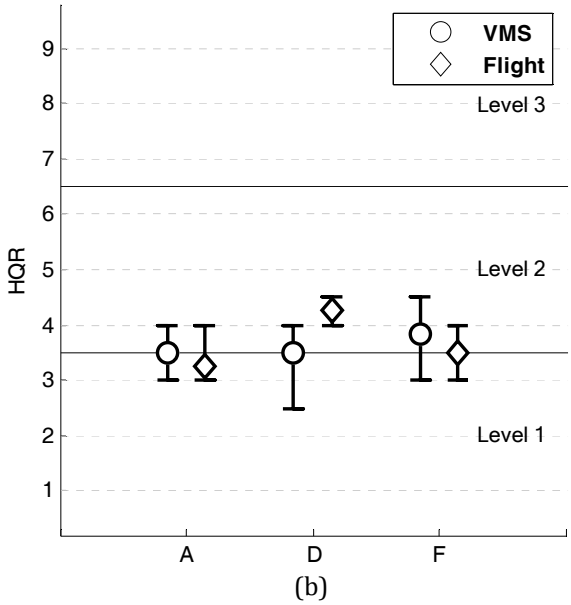

(b)

Figure 9: Comparison of Handling Qualities Ratings from VMS and flight testing (Hover MTE, Center Stick): (a) Rate Command, and (b) Attitude Command

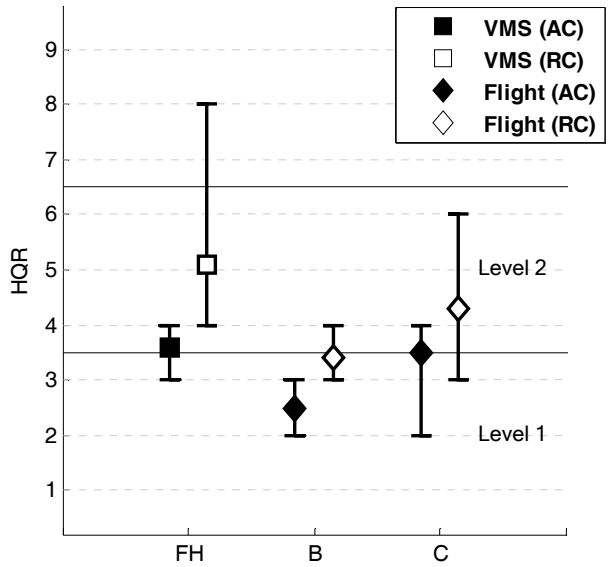

Figure 10: Handling Qualities Ratings for Hover MTE

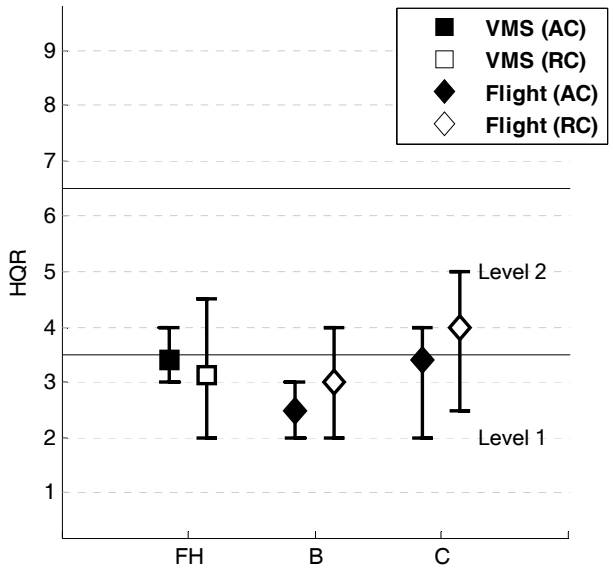

Figure 11: Handling Qualities Ratings for Slalom MTE

Shown in Figure 10 are the Handling Qualities Ratings for the Hover MTE evaluations of the force-feel configuration F_H, evaluated in the VMS only, and force-feel configurations B and C, evaluated in flight (Ref. 6). Results from the Slalom MTE evaluations of these same force-feel configurations are shown in Figure 11.

Configuration F_H was generally found to compare favorably with force-feel configuration A. With Attitude Command, both configurations in the VMS were consistently rated very similarly by the pilots in the Hover MTE, with F_H being assigned an average HQR 3.6 (Figure 10) and case A an HQR 3.4 (Figure 9(b)). Both cases with Rate Command were rated in Level 2. It is noted, however, that the rating for configuration F_H (average HQR 5.1) was heavily biased relative to case A (average HQR 4.3) by one pilot, from the five evaluation pilots that rated it in the VMS. General evaluation comments from the remaining four pilots did not indicate significant differences between the handling qualities of these two cases. Results for the Slalom MTE (Figure 11) show Attitude Command configuration F_H was less preferred, relative to case A. Comments for this configuration started to point to a loss in precision in capturing wings level attitude.

Pilot evaluation comments

Reference 6 provided a summary of the pilot comments describing the general characteristics for the various experimental force-feel configurations. Pilot comments from the VMS experiment largely tended to corroborate these assessments.

For the Hover MTE in general, higher damping allowed, and often required, the pilot to close the loop more tightly, without risk of PIO, in order to achieve the desired performance. One of the benefits of increased damping seemed to be that greater levels of precision were achieved resulting in the lowest workload. This would be characteristic of Case A. Lower damping, such as that of Cases F and D, often resulted in "overly sensitive" and "unpredictable" response characteristics conducive to a "definite tendency to over control".

The pilots perceived that the inceptor configurations with lower natural frequencies presented a heavier feel, and were less sensitive, making the workload to capture and maintain a hover more difficult. An inceptor with the combination of a heavy feel and low damping (configuration D) provided the least precision, felt wobbly when making small rapid inputs, and was the most prone to over-controlling the aircraft.

A more detailed examination of the pilot evaluation comments from the VMS experiment highlighted specific characteristics about the low damping force-feel configurations (i.e., F and D):

- An often noticeable difference between lateral and longitudinal control characteristics, with longitudinal controller feeling heavier compared to lateral, which was more prone to PIO/over control
- Low damping configurations were easily identified because they allowed high frequency inputs.

For the Slalom MTE, the overarching factors that affected pilot perception remain fundamentally the same – mainly how precisely the aircraft tracked or responded to control inputs. In particular, pilots had a marked preference for well damped configurations to prevent: (a) over-controlling that would results in jerky ride qualities, and (b) susceptibility to bio-feedback. It was noted that bio-feedback (aircraft vibrations being fed back through the pilot's arm into the inceptor) and its effect was more noticeable in the attitude command configuration since the lateral cyclic inputs had to remain displaced and held from the detent in order to hold the desired aircraft attitudes. The lighter, less-damped configurations (configurations C) proved to be the most susceptible to bio-feedback interference with the slalom task.

Inverse Dynamic Analysis

Crossover frequency estimation

Estimates of the inner-loop crossover frequencies from inverse dynamic analysis were obtained using the approximation of Eq. (2) for an inclusive combination of pilot model parameters and experimental force-feel configurations. Provided that stable solutions were achieved, differences in the various estimates were found to be fairly small (normally within ±0.05 rad/s). Resulting nominal values from this analysis are listed in Table 3 for both the Attitude and Rate Command response types and the Slalom and Hover MTEs.

Figure 12 shows the commanded trajectory computed by inverse dynamic procedure for the output to accurately track the desired path along the course. Note the relaxed entry and exit headings on the desired trajectory. Pilots were not enforced during testing to enter and leave the course parallel to the centerline, and therefore this condition was not applied in the analysis. This simulated slalom maneuver was conducted at 60 knots, which is representative of the minimum aggressiveness required while still achieving desired performance.

Figure 13 shows a desired groundspeed profile for the Hover MTE maneuver. The maneuver depicted was representative of a low aggressiveness flight profile, with the pilot holding a steady 6 knots velocity on the run in and decelerating into position in a stable hover in 5 seconds. The pilot model is seen here to track this profile effectively, despite the presence of gust disturbances. The main driver of the crossover frequency requirement was the deceleration time. Analysis of a hypothetical high aggressiveness scenario, defined by a 10-knot run-in and a 5-second deceleration, resulted in identical crossover frequencies. At the other extreme, a low aggressiveness deceleration of 8 seconds resulted in 1.2–1.4 rad/s crossover frequencies for both response types. Presence of turbulence forced increased control activity of the pilot model to maintain the hover within the specified performance requirements. This did not necessarily affect the crossover frequency estimate, but rather greatly improved the correlation of the cut-off frequencies from the Hover MTE analysis.

Table 3. Estimated crossover frequencies from inverse dynamic analysis

MTE	Response Type	Crossover Frequency (rad/s)	
		Roll	Pitch
Slalom	RC	1.4	N/A
	AC	1.4	N/A
Hover	RC	2.0	2.0
	AC	1.8	2.2

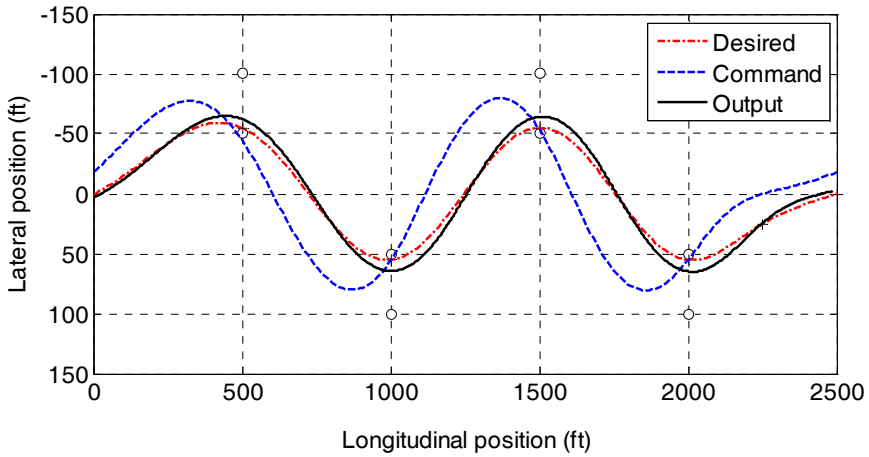

Figure 12: Ground track from inverse dynamic analysis for Slalom MTE (RC, baseline)

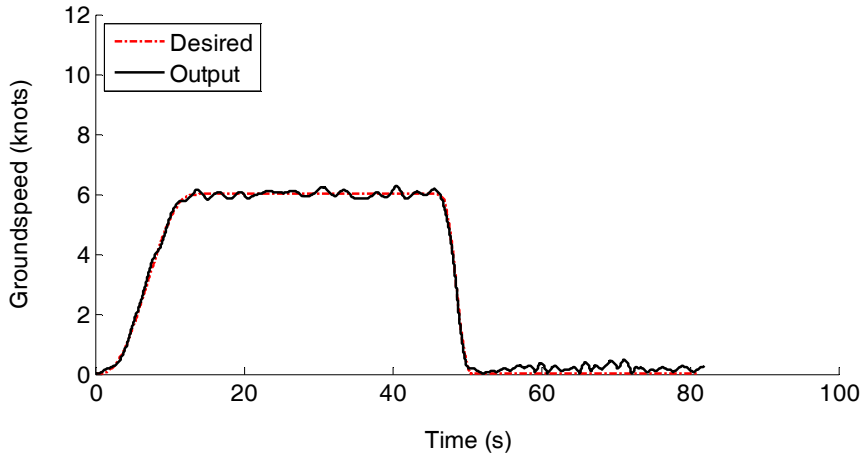

Figure 13: Groundspeed profile from inverse dynamic analysis for Hover MTE (AC, baseline)

Comparison with cut-off frequencies from flight

Spectral analysis of the model-generated control inputs indicated that crossover frequencies from Table 3 compared quite favorably with the cut-off frequencies, particularly to those from the Hover MTE simulation analysis (Figure 14). Analysis of the Hover MTE yielded cut-off frequencies in the 1.5–2.2 rad/s range in both axes. Cut-off frequencies computed from the slalom simulation analysis were of the order of 0.7 rad/s. Moreover, cut-off frequencies from this analysis were subsequently seen to compare favorably with the cut-off frequencies obtained from flight test data (Ref. 6).

Although approximate, the pilot model crossover frequency estimates obtained from the inverse dynamic analysis were therefore considered to be broadly representative of typical pilot operating frequencies. Consequently, the nominal values in Table 3 were used throughout the ensuing analysis to tailor the configuration of pilot/vehicle model to be task-specific to the Slalom or Hover MTEs

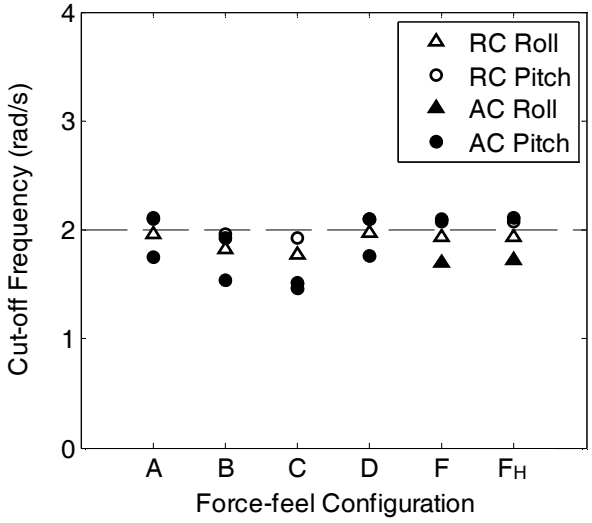

Figure 14: Cut-off frequencies from inverse dynamic analysis on the pilot model

Comparison with ADS-33 Design Criteria

Ref. 6 presented a preliminary comparison of design criteria of the lateral dynamics only in the Slalom MTE. This section will expand upon these findings by including improved aircraft models, and representative predictions for the Hover MTE, and a comparison of longitudinal dynamics.

Figure 15 shows the mapping of the five force-feel configurations of Ref. 6 into the short-term attitude response bandwidth and phase delay plot. These results are obtained from the attitude frequency response curves to force input, rather than displacement input. Results shown here are for the simplified LOES transfer functions of the aircraft, hence they differ slightly from those in Ref. 6. Handling qualities specification boundaries have been intentionally omitted from the chart. In Ref. 6 it had been shown there was a poor correlation of the experiment HQRs with the specified limits for UCE = 1 and fully attended operations. The following discussion focuses on the relative bandwidth and phase delay values of the various force-feel configurations to each other.

This mapping is of course a function of the gain and phase differences of the second-order approximation of the force-feel system relative to the frequency response to displacement input. Configurations A, D and F, with the low natural frequency, were clearly found to have a lower bandwidth and a higher phase delay than configurations B and C. This result was generally consistent with the experimental findings. Low damping ratios are seen to translate into a slight bandwidth increment, for a given natural frequency. The damping ratio is seen to have a different effect on the phase delay depending on the value of natural frequency. This is seen as an increase in phase delay in configuration D over A (low frequency configurations), but as a decrease in configuration C compared to B (high natural frequency configurations). Consequently, as indicated in Ref. 6, configuration C was consistently predicted to have the best handling qualities, based on the bandwidth and phase delay characteristics. Similarly, case A was theoretically found to consistently expect the worst, or near worst, handling qualities. These handling qualities predictions were, however, inconsistent with the piloted evaluation results, where case B was the most preferred and D the least preferred force-feel configuration.

Figure 16 shows the HQSF curves/plots for the Hover MTE, based on the estimates of crossover frequency obtained in the previous section. Only the longitudinal HQSF plots are shown for the hover analysis, since these indicated the worst predicted handling qualities. The HQSF plots are observed to be characterized by a primary peak near the crossover frequency and a secondary one, which as will be discussed further below, is known to be associated with the neuromuscular dynamics. The HQSF for force-feel cases D and F were omitted from Figure 16 for clarity, but these too displayed large peaks into the Level 3 region around the crossover frequency, with a magnitude between A and B.

Handling qualities predictions offered by the HQSF for the Hover MTE were observed to be overly pessimistic, failing to predict the assigned handling qualities from experiment. Predictions for the Slalom MTE fared slightly better, with results for the Attitude Command response type accurately predicting Level 1 handling qualities, and the predictions for the Rate Command being in the Level 1/Level 2 range. Of course, the specific prediction indicated by the HQSF is a function of crossover frequency and these predictions assume the estimated crossover frequencies are accurate indications of pilot control activity. Of interest in the subsequent discussion is how the HQSF results compare relative to each other.

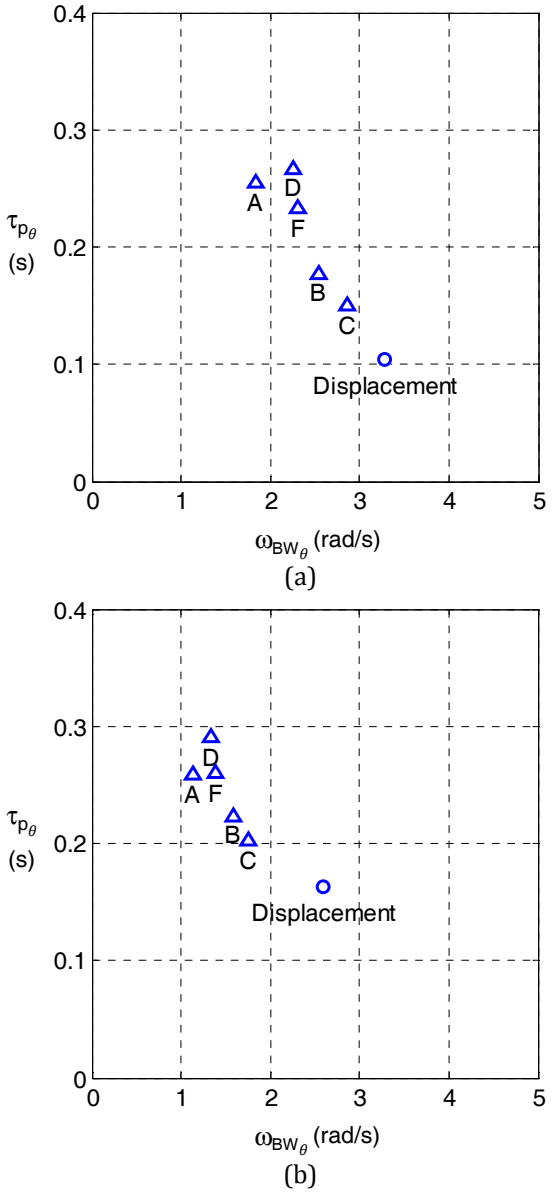

Figure 15: Short-term pitch response criteria to force input: (a) Attitude Command, and (b) Rate Command

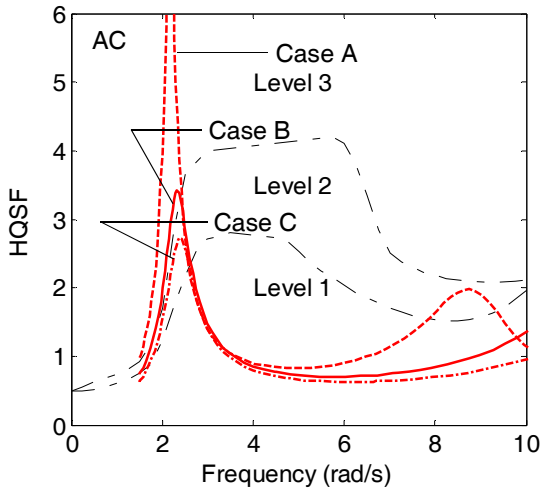

(a)

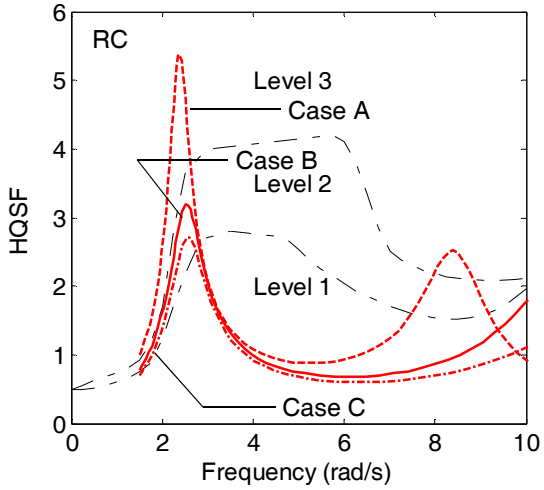

(b)

Figure 16: Handling qualities predictions based on HQSF for Hover MTE, longitudinal axis: (a) Attitude Command, and (b) Rate Command

Importantly, the HQSF plots in Figure 16 do mirror the trends illustrated by the bandwidth and phase delay maps in Figure 15. For example, case A was in theory predicted by the HQSF to have the worse handling qualities for both response types, inasmuch as it was characterized by the largest peak magnitude of the HQSF. Accordingly, case C was predicted to have the best handling qualities.

The HQSF peak observed near the crossover is a direct function of the phasing of the open-loop pilot/vehicle transfer function, and therefore is a direct reflection of its stability margins (Figure 17). Also exemplified in Figure 17 is the approximate $(\omega_c/s)e^{-\tau_e s}$ behavior of the crossover frequency model of the human pilot that is captured by the structural pilot model. Bandwidth and phase delay are, fundamentally, measures of the aircraft contribution to the stability margins in the pilot attitude loop closures. It is not surprising that handling qualities predictions from the structural model, being also governed by the classical crossover model of the pilot, agreed with the trends espoused by the short-term, small-amplitude input criteria.

Both methods effectively reflect the same information and therefore both approaches yield essentially equivalent comparative results between force-feel dynamics cases. Importantly, neither was shown to accurately predict the handling qualities, nor even the relative preferences indicated by the pilots.

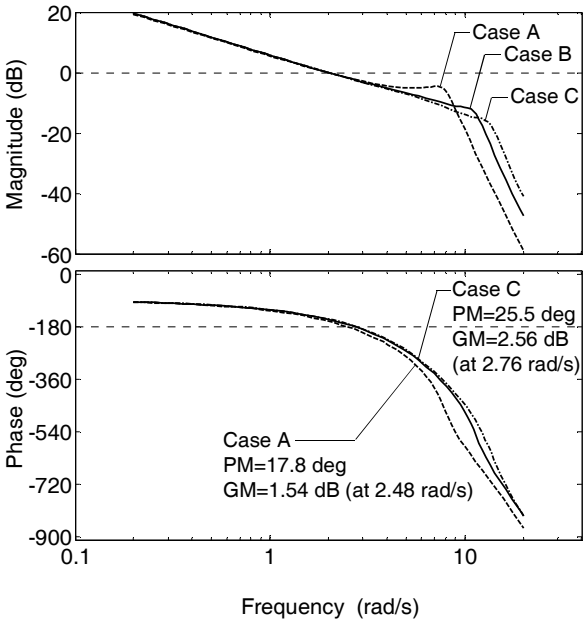

Figure 17: Open-loop pitch pilot/vehicle frequency response, Rate Command

Effect of Motion Feedback

As previously mentioned, the HQSF curves were characterized by a secondary peak observed in the higher frequency range (above 8 rad/s). This peak is known to be associated with the neuromuscular system dynamics and has been extensively studied in the context of closed-loop pilot/vehicle system phenomena such as PIO and roll ratcheting (Ref. 15). Pilot evaluation comments from the tests clearly indicated deficiencies with low damping force-feel configurations to be related with tendencies to over-control and susceptibility to biodynamic feedback.

This section will therefore present results of the examination of the effect of vestibular feedback and neuromuscular dynamics on the HQSF. Examination of the structural pilot model with vestibular feedback has not been reported in the literature. Although the subject of the mathematical modeling of pilot neuromuscular behavior in the context of aircraft inceptor force-feel dynamics has been studied extensively, e.g. in References 15 and 16, this particular methodology has also not been reported for neuromuscular dynamics other than the nominal second order characterization presented above. It was considered desirable to investigate the effect of said parameters on the HQSF curves before attempting the comparison with experimental results.

Effect of motion cues

Motion cues are well known to be crucial to the control of a helicopter in hover (Ref. 17). On the other hand, with a reasonable turn coordination it is expected the pilot will perceive minimal lateral accelerations associated with the rolling and turning of the aircraft as he or she executes the slalom course. It could be argued motion cues may play a minimal role in this case. Studying pilot evaluation comments, motion appeared in fact not to be a major factor. Pilot strategy was evidently heavily based on the "visual monitoring of the bank angles and the anticipation of the ensuing turn rate associated with these".

Cut-off frequencies from the spectral analysis of pilot station lateral acceleration measured from flight shown in Figure 18, supported the hypothesis that motion cues are lower in the Slalom MTE. Average values of the cut-off frequency for the Slalom MTE were found to be about half the value of those for the Hover MTE. Notwithstanding the frequency of the pilot station lateral accelerations, their amplitude in both the slalom and hover maneuvers was found to be small, with RMS values in the 0.02-0.05g range.

Incidentally, average values of the cut-off frequency for the Hover MTE evaluations are seen to be between 6 and 7 rad/s. By definition of the cut-off frequency this implies that half the power in the auto-spectrum is contained above this frequency. Therefore there must be a significant amount of frequency content of the measured accelerations overlapping with the frequency of the neuromuscular mode dynamics (8–10 rad/s).

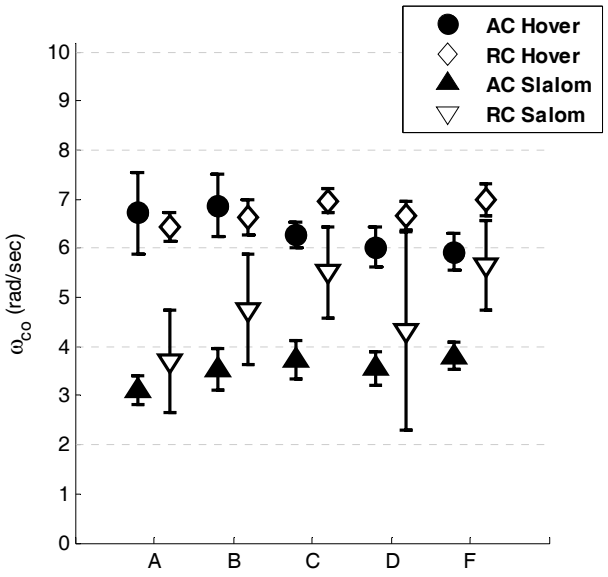

Figure 18: Cut-off frequencies for lateral accelerations at pilot station

Handling Qualities Ratings (HQR) in Table 4 indeed appeared to confirm a negligible influence of motion cues from the simulator in the execution and evaluation of the Slalom MTE. Similarly, from Table 4 it is seen that presence of motion cues in the simulation testing did improve the handling qualities from the Hover MTE, where motion provided a better ability to anticipate the drift of the aircraft. This improvement, while significant (roughly 1 HQR), was not sufficient to warrant a change in handling qualities Level, in this case. It does highlight, however, the necessity to consider the inclusion of vestibular feedback into the structural pilot model.

Table 4: Comparison of Handling Qualities Ratings from VMS with and without motion (RC, Case A)

	Hover		Slalom	
Pilot	**Motion**	**Fixed**	**Motion**	**Fixed**
1	3	4.5	2	2
2	5	7	4	4
3	5	5	3	3
4	4	6	3	2.5
Avg.	**4.3**	**5.6**	**3.0**	**2.9**

Vestibular feedback

Vestibular feedback provides in essence the ability to effect anticipatory response based on the physical sensing of accelerations. In other words, it provides lead to the pilot. To the pilot model it effectively provides the ability to execute derivative control, in addition to the proportional-integral action of the visual compensation model. In theory, so does the proprioceptive feedback, although through a very different mechanism. Vestibular feedback should, hypothetically, improve the ability of the pilot to control the aircraft. This should be reflected in the HQSF from the structural pilot model.

One direct effect of the vestibular gain on the model is to shift the 180-degree phase crossover frequency to higher frequencies relative to the gain crossover, consequently increasing the stability margins. This is evidenced in the frequency response of the inner-, open-loop transfer function as shown in Figure 19. This in turn is reflected in the HQSF by the reduction and slight shifting of the peak typically observed around the 2 rad/s (i.e., crossover) frequency (Figure 20). According to the theory behind the structural model, this reduction in the HQSF peak near 2 rad/s is suggestive of a reduction in the power of the proprioceptive compensation, which would dictate an improvement in the handling qualities.

The proprioceptive feedback gain is tuned according to the structural pilot model configuration procedure described in Ref. 11 to ensure a minimum damping ratio (i.e., 0.15) of the closed-loop proprioceptive system. Simply introducing vestibular feedback in parallel to the proprioceptive feedback has the effect of reducing the stability of this loop, potentially destabilizing it. This is manifested in Figure 19 for $K_{\dot{\phi}}$ greater than 0.12.

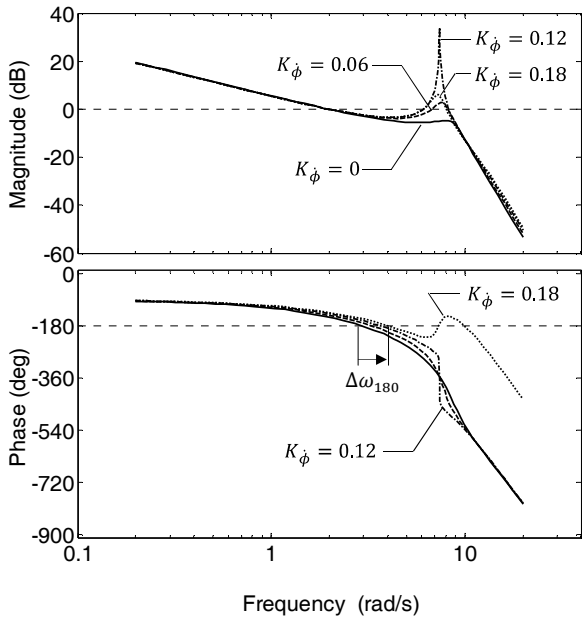

Figure 19: Open-loop pilot-vehicle roll axis transfer function for baseline, RC (2.0 rad/s crossover)

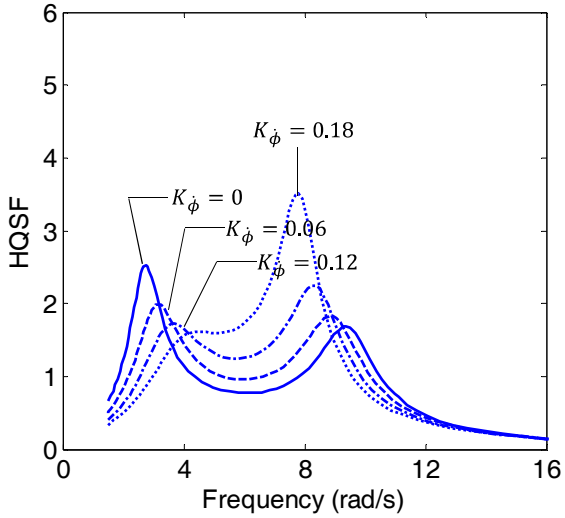

Figure 20: Effect of vestibular gain on HQSF for roll axis, baseline, Rate Command

This result is possibly academic, since pilots may not realistically destabilize the neuromuscular system in this fashion. In reality, this could result in the pilot being forced to reduce his or her gain in order to maintain adequate gain and phase margins. Effectively, this infers that motion feedback may induce the pilot into over-control through the fundamental physiological coupling of the neuromuscular system and the force-feel system. It is noted that this behavior is indicative of the resonant tendency contributed by the pilot identified in Ref. 15.

Results from Figure 19 showed that without any other adjustments to the model, increased vestibular gain tended to excite this resonant tendency. This open-loop resonant peak associated with the neuromuscular system was consequently found to be reflected in the secondary peak seen in the HQSF plots (Figure 20). Although the distance between the magnitude curve at the peak frequency and the 0 dB line in Figure 19 is reduced, the phase of the open-loop pilot-vehicle transfer function at the natural frequency of neuromuscular dynamics is typically sufficiently large that the required conditions for instability are not satisfied. Depending on the specific phasing of the open-loop pilot/vehicle transfer function the magnitude variation on the HQSF can be more or less pronounced.

The significance of this analysis is that handling qualities improvements predicted by the HQSF in the vicinity of the crossover frequency may thusly be lessened by the increased magnitude at the neuromuscular modal frequency, which has been argued could be related to a real tendency to over-control.

A variation (i.e., root locus) analysis of the vestibular feedback gains was conducted with the nominal configuration parameter values in place and the proprioceptive loop closed. Indicated by the lower values of the vestibular feedback gain allowed before reaching the point of instability, results shown in Figure 21 suggest that force-feel configurations D and F should be the more susceptible to any pilot compensation that may be induced by aircraft motion. Following through with this argument, lateral (roll) dynamics were also found to be the more sensitive to vestibular feedback, and of the two response types in the roll axis, Attitude Command was seen to be the most sensitive.

These observations are significant in that they suggest that inceptor damping plays a crucial role in the sensitivity of the pilot model to vestibular feedback. More to the point, they suggest that low damping ratios of the inceptor make the model less tolerant to the potential compensation that could be elicited by the pilot in response to motion, and consequently more prone to over-control.

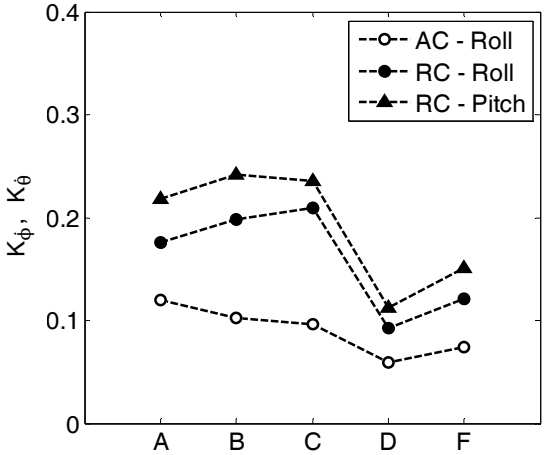

Figure 21: Vestibular feedback gain for neutral stability of the neuromuscular mode

Neuromuscular components

The prior discussion has highlighted the significance of neuromuscular dynamics in the effect of vestibular feedback on the HQSF. Additionally, it could be argued that the effects of the different restraints on the pilot arm between the center-stick and side-arm configurations could, hypothetically, be represented by variations in the neuromuscular model. Therefore it was of some interest to investigate the potential effect these neuromuscular dynamics parameters had on the HQSF.

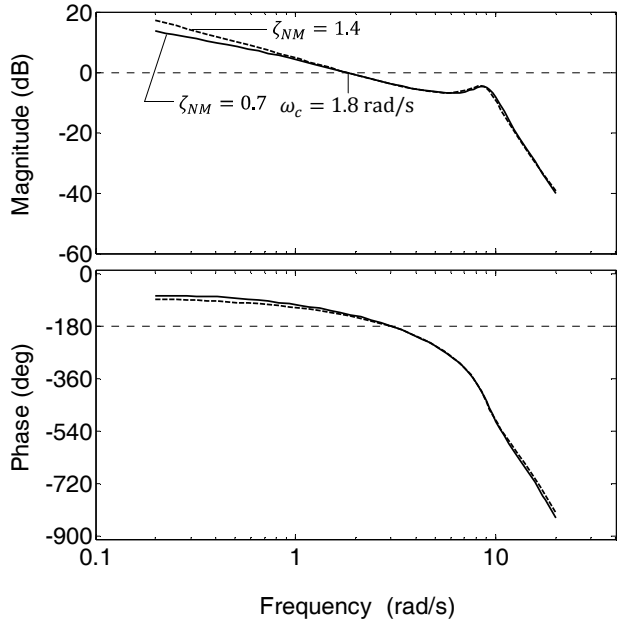

Figure 22: Open-loop $Y_{P_\phi} Y_\phi$ frequency response for varying neuromuscular damping ratios, baseline, AC

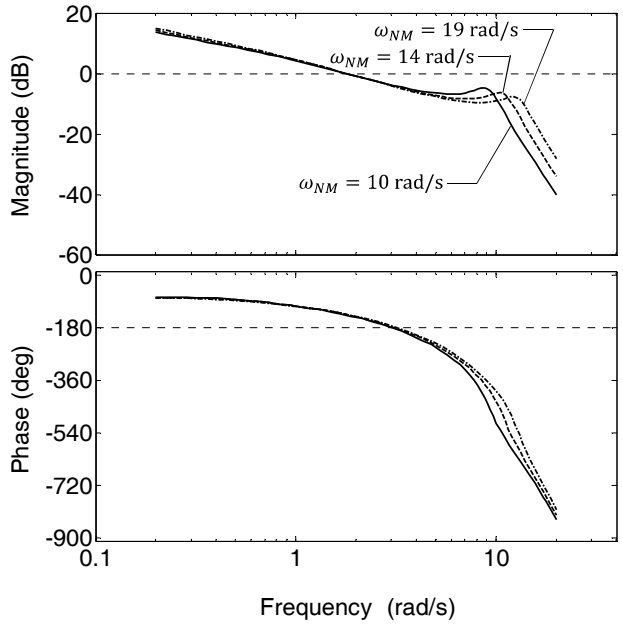

Figure 23: Open-loop $Y_{P_\phi} Y_\phi$ frequency response for varying neuromuscular frequency, baseline, AC

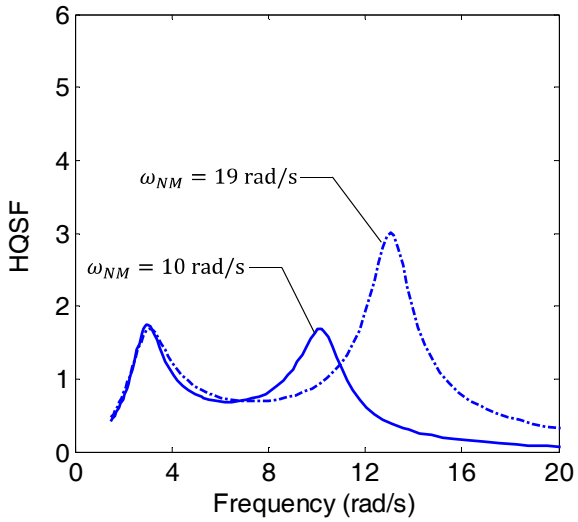

Figure 24: Effect of neuromuscular damping ratio on baseline AC roll control HQSF

Variation in the damping ratio of the neuromuscular system was seen to have a very small effect on the neuromuscular mode resonance peak of the baseline Attitude Command configuration (case F). The pilot model was of course programmed to "adapt" to the increased neuromuscular damping by increasing the proprioceptive gain in order to achieve the desired 0.15 minimum damping ratio of the proprioceptive closed-loop system. The net effect is seen in Figure 22 only as a slight variation in the pilot gain and phase in the low frequency region (below 1 rad/s). This would require an adjustment to the integral compensation gain in order to recover the proper ω_c/s behavior, with its resulting effects on the HQSF. With the increased damping an overall increase of the proprioceptive compensation, and hence the HQSF, over the entire frequency range was obtained. The unseen benefit of increasing the damping ratio of the neuromuscular system is that it makes it much less sensitive to vestibular feedback. Vestibular feedback gain can be increased to significantly higher values without the stability of the system being affected drastically, hence also indicating the pilot would be less prone to over-control based on the arguments from the previous section.

The neuromuscular natural frequency was found, however, to have a noticeable effect on the positioning of the neuromuscular resonance peak (Figure 23) and consequently also on the associated secondary peak in the HQSF of the roll loop (Figure 24). The resulting elevated peak for the 19 rad/s neuromuscular frequency would indicate a heighted sensitivity to any kind of high frequency aircraft roll requirements, and would be an undesirable characteristic.

Summary Discussion

Comparison of analytical handling qualities predictions with experimental test results confirmed the HQSF failed, for some of the configurations, to correlate with the

assigned HQR, when employing the nominal parameters. This result is of course subject to the crossover frequencies employed in the analysis. Since accuracy of the crossover frequency estimates from the inverse dynamic analysis was not in question, these boundaries may need to be reexamined, to include vestibular feedback.

Rather than dwelling on the specific validation of this set of boundaries, the subsequent analysis of the effect of the force-feel dynamic characteristics focused on the relative differences in the HQSF between configurations. The comparative trends from the HQSF analysis was contrasted to the ADS-33 short-term attitude design criteria, but applied to the force input. The relative predictions between configurations were found to mirror each other, since both metrics fundamentally are direct reflections of the stability margins of the open-loop pilot/vehicle attitude transfer function.

An exhaustive examination of the pilot/vehicle model, for varying combinations of vestibular feedback and neuromuscular dynamics was conducted. This analysis revealed a significant sensitivity of the pilot model to aircraft motion for the force-feel configurations with reduced damping. This behavior was associated with the increasing magnitude of the open-loop resonant peak associated with the neuromuscular system. Of course, this behavior was also determined to be highly dependent on the phase of the open-loop pilot/vehicle transfer function at this frequency.

While a formal PIO analysis was not conducted, this heightened sensitivity of the pilot model to aircraft motion was likened to a propensity to PIO by the pilot. Force-feel configurations with the low damping and natural frequency (D and F) were found to be the most sensitive. This result was found to be consistent with piloted evaluations, whereas the nominal analysis could not predict this behavior.

Increasing the natural frequency of the force-feel dynamics had the effect of shifting the resonance peak to a higher frequency, and thus reducing its impact on the HQSF in the frequency range associated with handling qualities (1.5–10 rad/s). However, in doing so made the configuration potentially more prone to biodynamic-feedback in response to high frequency aeroelastically-induced vibration. This could explain this propensity for force-feel configuration C.

Design requirements defining inceptor force-feel dynamic characteristics therefore cannot be formulated in isolation. The coupled nature of the inceptor and aircraft response dynamics needs to be considered, inasmuch as they have a significant impact on the magnitude and phase of the open-loop pilot/vehicle transfer function at the neuromuscular mode frequency. Conservative design of force-feel characteristics should ensure low natural frequency and low damping combinations be avoided as they were shown to be prone to PIO in both analysis and experiment.

Finally, it is noted that analysis centered on the results for a center stick inceptor, but certain assertions for the side-arm controller may be inferred from the parametric analysis of the neuromuscular dynamic characteristics. This analysis showed how a hypothetical increase in the damping of the neuromuscular model significantly reduced the sensitivity of the proprioceptive loop to vestibular feedback. If the argument that side-arm restraints is somehow to increase the neuromuscular system damping is accepted, then the reduced influence of inceptor damping on the handling qualities for the side-arm configurations would be easily explained.

Conclusions

Based on the analysis of results from the systematic examination of the structural pilot model and the flight and simulation test piloted evaluations presented above, it is possible to establish the following conclusions:

1) Qualitative analysis of the relative effects on the handling qualities of different force-feel dynamics is possible using a well-defined pilot/vehicle model based on the basic principles espoused by the classical crossover pilot model theory.

2) Where vestibular feedback plays a significant role, it is possible to correlate the analysis with flight and simulation results.

3) The fundamental effect of force-feel dynamics on the handling qualities is characterized by the effect it has on the gain and phase properties of the pilot/vehicle open-loop resonance peak associated with the neuromuscular system.

Acknowledgements

The authors would like to thank Prof. Ron Hess from UC Davies for his insight in implementing the structural pilot model and interpreting its results.

References

[1]Landis, K., and Glusman, S., "Development of ADOCS controllers and control laws: Vols 1-3". *USAAVSCOM TR 84-A-7*, March 1987.

[2]Watson, D. C., and Schroeder, J. A. "Effects of Stick Dynamics on Helicopter Flying Qualities," *AIAA-90-3477-CP*, Presented at the AIAA Guidance, Navigation and Control Conference, August 1990.

[3]Mitchell, D. D., Aponso, B. L., and Klyde, D. H., "Feel Systems and Flying Qualities". *AIAA-95-3425-CP*, Presented at the AIAA Atmospheric Flight Mechanics Conference, Baltimore, MD, Aug. 7-10, 1995.

[4]Morgan, M. J., "An Initial Study into the Influence of Control Stick Characteristics on the Handling Qualities of

a Fly-By-Wire Helicopter," *AGARD-CP-508*, February, 1991.

[5]Greenfield, A., and Sahasrabudhe, V., "Side-Stick Force-Feel Parametric Study of a Cargo-Class Helicopter," *Proceedings of the 67th annual forum of the American Helicopter Society*, Virginia Beach, VA, May 3-5, 2011.

[6]Lusardi, J.A., et al. "In Flight Evaluation of Active Inceptor Force-Feel Characteristics and Handling Qualities,". *Proceedings of the 68th Annual Forum of the American Helicopter Society*, Phoenix, AZ, May, 2012.

[7]von Grünhagen, W., Schönenberg, T., Lantzsch, R., Lusardi, J.A., Lee, D., and Fischer H., "Handling Qualities Studies into the Interaction Between Active Sidestick Parameters and Helicopter Response Types," Presented at the 38th European Rotorcraft Forum, Amsterdam, the Netherlands, September 4-7, 2012

[8]Anon., "Handling Qualities Requirements for Military Rotorcraft, ADS-33E-PRF". U.S. Army Aviation and Missile Command, Mar, 2000.

[9]Hess, R. A., "Analyzing Manipulator and Feel System Effects in Aircraft Flight Control," *IEEE Transactions on Systems, Man and Cybernetics*, Vol. 20, (4), July/August 1990, pp. 923-931.

[10]Hess, R. A., "Unified Theory for Aircraft Handling Qualities and Adverse Aircraft-Pilot Coupling," *Journal of Guidance, Control and Dynamics,* Vol.20, (6), 1997, pp. 1141-1148.

[11]Hess, R. A., Zeyada, Y., and Heffley, R. K. "Modeling and Simulation for Helicopter Task Analysis," *Journal of the American Helicopter Society,* Vol. 47, (4), October 2002, pp. 243-252.

[12]Heffley, R. K., Bourne, S. M., and Hindson, W. S., "Helicopter Pilot Performance for Discrete-Maneuver Flight Tasks," *Proceedings of the Twentieth Annual Conference on Manual Control, NASA Conf. Pub. 2341,* June 1989, pp. 223-231.

[13]Aponso, B. L., Tran, D. T., Schroeder, J. A., and Beard, S. D., "Rotorcraft Research at the NASA Vertical Motion Simulator," *AIAA-2009-6056*, Presented at the AIAA Atmospheric Flight Mechanics Conference, Chicago, IL, Aug. 10-13, 2009.

[14]Lusardi, J. A., von Gruenhagen, W., and Seher-Weiss, S., "Parametric Turbulence Modeling for Rotorcraft Applications, Approach, Flight Tests and Verification," *Proceedings of the Rotorcraft Handling Qualities Conference*, University of Liverpool, UK, Nov. 2008.

[15]Johnston, Donald. E., and Aponso, Bimal. L., "Design Considerations of Manipulator and Feel System Characteristics in Roll Tracking," *NASA CR-4111*, Feb. 1988.

[16]McRuer, D. T., and Krendel, E. S., "Mathematical Models of Human Pilot Behavior," *AGARD-AG-188*, Jan. 1974

[17]Schroeder, J. A., and Grant, P. R., "Pilot Behavioral Observations in Motion Flight Simulation," *AIAA 2010-8353*, Presented at the AIAA Modeling and Simulation Technologies Conference, Toronto, Ontario Canada, August 2–5, 2010